Polymerization of Sulfopropyl Methacrylate, a Surface Active Monomer, within Layered Double Hydroxide

Claudia Roland-Swanson, Jean-Pierre Besse, and Fabrice Leroux*

Laboratoire des Matériaux Inorganiques, UMR 6002-CNRS, Université Blaise Pascal, 24 av. des Landais, 63177 Aubière cédex, France

Received April 5, 2004. Revised Manuscript Received September 21, 2004

Hybrid organic−inorganic phases composed of a surface active monomer, sulfopropyl methacrylate (SPMA), incorporated within the lamellar structure of layered double hydroxides (LDH) of cation composition Zn_nAl, $n = 2, 3$ are obtained by the coprecipitation method. Monomer intercalation and its subsequent polymerization are characterized by means of FTIR and ^{13}C CP-MAS NMR spectroscopies. Complementary information was gathered from a thermal study of the potassium salt of SPMA. In-situ X-ray diffraction over a range of temperature performed on the hybrid phase Zn_2Al/SPMA shows clearly that the polymerization process is found first to slightly contract and then to disagglomerate the lamellar structure, while the integrity of the layers is maintained, giving rise to well-dispersed particles.

1. Introduction

Inorganic−organic hybrid materials have received a lot of attention for the past 10 years.[1] The possibility to combine the properties of the two components has been the driving force in numerous fields of application.

For the inorganic framework, we are interested in layered double hydroxide (LDH) materials. Namely, LDH-type materials present a large versatility in terms of chemical composition and layer charge, and find potential application in numerous domains such as in green chemistry,[2] as precursors of catalysts,[3] etc. The LDH structure is referred to the natural hydrotalcite, and described with the ideal formula $[M^{II}_xM_{1-x}{}^{III}(OH)_2]_{intra}[A^{m-}_{x/m}\cdot nH_2O]_{inter}$, where M^{II} and M^{III} are metal cations, A is the anions, and *intra* and *inter* denote the intralayer and interlayer domains, respectively. The structure consists of brucite-like layers of edge-sharing $M(OH)_6$ octahedra. Partial M^{II} to M^{III} substitution induces a positive charge for the layers, balanced with the presence of the interlayered anions.

Hybrid LDH materials composed of macromolecules as the organic moiety have been extended from the incorporation of biomolecules such as nucleoside monophosphate,[4] or biopolymer such as alginate,[5] to the uptake of monomer molecules. For the latter, few review articles are devoted to the intercalation and in-situ polymerization process.[6] Up to now, monomers with acrylate or vinyl polymerizable function were mostly studied. However, one has to note the intercalation−polymerization of poly(α, β aspartate) which proceeds by the condensation from the aminosuccinic acid via a polysuccinimide intermediate.[7] Concerning monomers with vinyl function, most of the previous studies relate the direct incorporation of polymer within LDH interlayer space.[8] Alternatively, we have shown recently that the in-situ polymerization of styrene sulfonate may be thermally induced into a non-oxidizing LDH structure such as LDH material of cation composition Zn_2Al[9] and hydrocalumite[10] host frameworks.

Some works report also the photopolymerization of 4-vinylbenzoate and *m*- and *p*-phenylenediacrylates (PDA) in hydrotalcite interlayers.[11] A cycloaddition was found to occur between adjacent PDA molecules; the authors surmise that it gives rise to a trans zigzag organic interlayer structure. Additionaly, aniline-[12] and pyrrole[13]-based monomers were also incorporated within LDH gap.

Concerning acrylate-based monomer, Tanaka et al. demonstrated that organic−inorganic interstratified materials may be obtained by exchange of nitrate LDH

* To whom correspondence should be addressed. E-mail: fleroux@chimtp.univ-bpclermont.fr.

(1) *Chem. Mater*. **2001**, *13* (10; Special Issue on Organic−Inorganic Nanocomposite Materials).

(2) Inacio, J.; Taviot-Guého, C.; Forano, C.; Besse, J.-P. *Appl. Clay Sci.* **2001**, *18*, 255.

(3) Vaccari, A. *Appl. Clay Sci.* **1999**, *14*, 161.

(4) Choy, J.-H.; Kwak, S.-Y.; Park, J.-S.; Jeong, Y.-J.; Portier, J. *J. Am. Chem. Soc*. **1999**, *121*, 1399.

(5) Leroux, F.; Gachon, J.; Besse, J.-P. *J. Solid State Chem*. **2004**, *177*, 245.

(6) Duguet, E.; Rey, S.; Merida Robles, J. M. In *Encyclopedia of Polymer Science and Technology*; John Wiley & Sons: Hoboken, NJ, 2003. Leroux, F.; Besse, J.-P. *Chem. Mater.* **2001**, *13*, 3507. Leroux, F.; Besse, J.-P. In *Clay Surfaces: Fundamentals and Applications*; Wypych, F., Satyanarayana, K. G., Eds.; Elsevier: New York, 2004; Vol. 1, Chapter 16, (ISBN 0120884399).

(7) Whilton, N. T.; Vickers, P. J.; Mann, S. *J. Mater. Chem*. **1997**, *7*, 1623.

(8) Messersmith, P. B.; Stupp, S. I. *Chem. Mater*. **1995**, *7*, 454. Oriakhi, C. O.; Farr I. V.; Lerner, M. M. *Clays Clay Miner*. **1997**, *45*, 194. Wilson, O. C., Jr.; Olorunyolemi, T.; Jaworski, A.; Borum, L.; Young, D.; Siriwat, A.; Dickens, E.; Oriakhi C.; Lerner, M. M. *Appl. Clay Sci.* **1999**, *15*, 265. Oriakhi, C. O.; Farr I. V.; Lerner, M. M. *J. Mater. Chem*. **1996**, *6*, 103.

(9) Moujahid, El M.; Besse, J.-P.; Leroux, F. *J. Mater. Chem.* **2003**, *13*, 258.

(10) Vieille, L.; Taviot-Guého, C.; Besse, J.-P.; Leroux, F. *Chem. Mater.* **2003**, *15*, 4369. Vieille, L.; Moujahid, El M.; Taviot-Guého, C.; Besse, J.-P. Leroux, F. *J. Phys. Chem. Solids* **2004**, *65*, 385.

(11) Shichi, T.; Yamashita, S.; Takagi, K. *Supramol. Sci*. **1998**, *5*, 303.

10.1021/cm040165x CCC: $27.50
Published on Web 11/11/2004

phase with the addition of an initiator at 80 °C; the interlayer acrylate anions were polymerized to form a hydrotalcite−poly(acrylate) intercalation compound.[14] A similar route was also used for the polymerization of acrylate into Ni-based LDH materials deriving from $Ni(OH)_2$.[15] More recently, the same group has shown that monomer intercalation and its subsequent polymerization have appeared to be strongly dependent upon the nature of the substituting cation M in the slabs of $Ni_{\approx 0.70}M$. Free-radical polymerization has been successfully initiated by sodium persulfate with heat for M = Fe, whereas for M = Co and Mn a one-step intercalation polymerization seems to occur.[16] The spontaneous polymerization is explained to occur not via the reductive intercalative process (RIP) as observed for xerogel V_2O_5 host matrix[17] but rather by an electron-transfer initiation from the mineral leading of a radical anion.[18] Additionally, the hybrid preparation strongly influences the arrangement of the anions, giving rise to either bilayer or monolayer of the poly(acrylate) macromolecules. In some cases, sulfate anions coming from the initiator are not avoided between the layers. The authors have shown that a thermal treatment at 60 °C for 24 h does not induce the in situ polymerization.

We focus our attention on the incorporation of acrylate-based surface active monomer into LDH gap to make the whole structure compatible towards polymer for its potential application as nanofiller. In the early 1990s, the group of Lagaly had extensively studied the incorporation of anionic surfactants and other fatty acids.[19] Depending on their nature, monomolecular films of high regularity or strongly tilted from the hydroxide sheets or formation of bilayer of surfactant molecules may be obtained within LDH gap. To our knowledge, it is the first time that surfactant molecules presenting a polymerizable function are incorporated into LDH structure. Commercially available sulfopropyl methacrylate is a good candidate as organic moiety since the presence of a highly hydrophilic sulfonate group would be attractive for the LDH sheets. Also the hydrophobic part and the presence of a double bond C=C should be an advantage for the hybrid material to interact strongly with a polymer matrix after the polymerization process, thus immobilizing the structure, and therefore being potentially beneficial for the enhancement of the mechanical properties.[20] Recently studied for such an application, LDH organo-modified materials dispersed into polyimide[21] and epoxy[22] polymer matrixes were found to provide enhanced properties to the nanocomposites.

SPMA was used as comonomer for the preparation of latex particles of poly(styrene co-butylacrylate) by emulsion polymerization, and the authors found that the particle diameters decrease with increasing SPMA concentration at constant ionic strength.[23] Copolymer nanoparticles prepared by free radical polymerization of SPMA were also studied for their efficiency to load hydrophilic drugs.[24]

Since, in our case, the electron-transfer mechanism from the host structure is not possible and the use of initiator may induce contamination, a soft heat treatment was used for the polymerization of SPMA constrained into LDH structure. The samples are characterized by means of XRD performed in situ with heat, thermogravimetric analyses, FTIR and ^{13}C CP-MAS NMR spectroscopies, and transmission electron microscopy.

2. Experimental Section

2.1. Preparation of the Samples. $ZnCl_2 \cdot 5H_2O$ (Acros), $Al(NO_3)_3 \cdot 9H_2O$ (Acros, 99%), NaOH (Acros, 97%), and 3-sulfopropyl methacrylate potassium salt (SPMA, $H_2C{=}C(CH_3)CO_2(CH_2)_3SO_3K$) (98%, Aldrich) were used as received.

The hydrotalcite-like materials were prepared by the coprecipitation method according to Miyata.[25] Experimentally, 250 mL of a solution of the salts Zn^{II}(10^{-2} M) and Al (5×10^{-3} M) was added dropwise to a solution containing SPMA (1.5×10^{-2} M) under nitrogen atmosphere.

The pH was kept constant at 10 ± 0.1 during the addition. The slurry was aged overnight, centrifuged, and then washed several times with distilled water, and finally dried at room temperature. The thermal treatment to induce the polymerization process was carried out at 200 °C for 2 h in a tubular oven under a flow of air.

Elemental analysis (H, C, S, Zn, and Al) was performed at the Vernaison Analysis Center of CNRS using inductive conduction plasma coupled to atomic emission spectroscopy (ICP/AES).

2.2. Techniques of Characterization. Powder X-ray diffraction profiles (PXRD) were obtained with a Siemens D501 X-ray diffractometer with a diffracted beam monochromator Cu Kα source. Powder X-ray diffraction (PXRD) profiles were obtained over a range of temperatures with a Philips X'Pert Pro diffractometer using Cu Kα radiation and equipped with a HTK16 Anton Paar chamber and a PSD-50m Braun detector (aperture on 2°, 155 channels). Measurements were carried out under a flow of air in the temperature range 20−500 °C, after 30 min equilibration at each temperature, and the heating rate was 60 °C/min. Typical measurement conditions were in the 2θ range 2−70°, step size 0.05° (2θ), and step counting time 20 s.

FTIR spectra were recorded on a Perkin-Elmer 2000 FT spectrometer employing the KBr dilution technique. Thermogravimetric (TG) analyses were performed under air atmosphere on a Setaram TGA 92 instrument using a linear slope for the heating rate of 10 °C/min.

2.3. Solid-State NMR Spectroscopy. ^{13}C ($I = {}^1/_2$) solid-state NMR experiments were performed with a Bruker 300 spectrometer at 75.47 MHz, using magic angle spinning (MAS) condition at 10 kHz and a 4-mm diameter zirconia rotor. ^{13}C

(12) (a) Challier, T.; Slade, R. C. T. *J. Mater. Chem*. **1994**, *4*, 367. (b) Isupov, V. P.; Chupakhina, L. E.; Ozerova, M. A.; Kostrovsky, V. G.; Poluboyarov, V. A. *Solid State Ionics* **2001**, *141*−*142*, 231. (c) El Moujahid, M.; Dubois, M.; Besse, J.-P.; Leroux, F. *Chem. Mater.* **2002**, *14*, 3799.

(13) Tronto, J.; Sanchez, K. C.; Crepaldi, E. L.; Naal, Z.; Klein, S. I.; Valim, J. B. *J. Phys. Chem. Solids* **2004**, *65*, 493.

(14) Tanaka, M.; Park, I. Y.; Kuroda, K.; Kato, C. *Bull. Chem. Soc. Jpn*. **1989**, *62*, 3442.

(15) Rey, S.; Mérida-Robles, J.; Han, K.-S.; Guerlou-Demourgues, L.; Delmas, C.; Duguet, E. *Polym. Int*. **1999**, *48*, 277.

(16) Vaysse, C.; Guerlou-Demourgues, L.; Duguet, E.; Delmas, C. *Inorg. Chem*. **2003**, *42*, 4559.

(17) Kanatzidis, M. G.; Wu, C.-G.; Marcy, H. O.; DeGroot, D. C.; Kannewurf, C. R. *Chem. Mater.* **1990**, *2*, 222. Liu, Y.-J.; DeGroot, C. D.; Schindler, J. L.; Kannewurf, C. R.; Kanatzidis, M. G. *J. Chem. Soc., Chem. Commun.* **1993**, 688.

(18) Vaysse, C.; Guerlou-Demourgues, L.; Delmas, C.; Duguet, E. *Macromolecules* **2004**, *37*, 45.

(19) Kopka, H.; Beneke, K.; Lagaly, G. *J. Colloid Interface Sci*. **1988**, *123*, 427. Meyn, M.; Beneke, K.; Lagaly, G. *Inorg. Chem*. **1990**, *29*, 5207.

(20) Strawhecker, K. E.; Manias, E. *Chem. Mater*. **2000**, *12*, 2943.

(21) Hsueh, H. B.; Chen, C.-Y. *Polymer* **2003**, *44*, 1151.

(22) Hsueh, H. B.; Chen, C.-Y. *Polymer* **2003**, *44*, 5275.

(23) André, A.; Henry, F. *Colloid Polym. Sci*. **1998**, *276*, 1061.

(24) Langer, K.; Stieneker, F.; Lambrecht, G.; Mutschler, E.; Kreuter, J. *Int. J. Pharm.* **1997**, *158*, 211. Langer, K.; Marburger, C.; Berthold, A.; Kreuter, J.; Stieneker, F. *Int. J. Pharm.* **1996**, *137*, 67.

(25) Miyata, S. *Clays Clay Miner*. **1983**, *31*, 305.

Table 1. Chemical Analysis of Hybrid Materials Zn_nAl/SPMA (n = 2, 3) and the Relative d spacings. Chlorine Form of Zn_2Al Is Also Reported for Comparison

sample	chemical formula	d-spacing (nm)
Zn_2Al/Cl	$Zn_{0.67}Al_{0.33}(OH)_2Cl_{0.33}\cdot 1.07H_2O$	0.78
Zn_2Al/SPMA	$Zn_{0.67}Al_{0.33}(OH)_2(H_2C{=}C(CH_3)CO_2(CH_2)_3SO_3)_{0.32}\cdot 1.33H_2O$	1.87
Zn_3Al/SPMA	$Zn_{0.76}Al_{0.25}(OH)_2(H_2C{=}C(CH_3)CO_2(CH_2)_3SO_3)_{0.24}\cdot 1.38H_2O$	1.87

spectra obtained by proton- enhanced cross-polarization method (CP) are referenced to the carbonyl of the glycine calibrated at 176.03 ppm.

2.4. Transmission Electronic Microscopy (TEM). TEM images were obtained by using a JEOL JEM-1200 operating at an acceleration voltage of 80 kV. The TEM samples were ultrasonically dispersed in ethanol and then a suspension was deposited onto holey carbon film deposited on a Cu grid.

3. Results and Discussion

3.1. Incorporation of the Surface Active Monomer. The chemical compositions are reported in Table 1. For both compositions, the molar ratios Zn to Al and Al to S are close to the expected values, i.e. close to the initial input ratio Zn/Al for the former (2 or 3); the relative amount in trivalent cations is directly related to the positive layer charge, which is then counterbalanced by the presence of the monofunctional anion SPMA, a ratio Al/S close to 1 is expected for the latter. The chemical formulas obtained from the elemental analyses indicate that the formation of LDH was complete and that the amount of SPMA, calculated from the sulfur content, is in agreement with what should be expected theoretically from an exchange capacity for the two host structures. One should note that any attempt to prepare a hybrid phase with lower aluminum content (n greater than 3 in Zn_nAl) was unsuccessful. The amount of water molecules is of the same amplitude as observed for other LDH hybrid materials[9] and includes the intercrystalline and interlayer components.

The XRD pattern of the hybrid phases exhibit features typical of LDH structure, which is generally described in $R\bar{3}m$ rhombohedral symmetry (Figure 1). In this structural description, the position of the diffraction line (110) is related to the cell parameter $\boldsymbol{a}$ by the relation $\boldsymbol{a} = 2{\cdot}d_{110}$. This diffraction line located at ≈60° is shifted between the two hybrid phases: 0.3054 and 0.3070 nm for n equal to 2 and 3 in Zn_nAl, respectively. Considering an ideal in-plane edge-sharing octahedra assembly, the cell parameter $\boldsymbol{a}$ is function of the ionic radii by the relation $\delta a/\delta n = -\sqrt{2}[r(Zn^{2+}) - r(Al^{3+})]$.

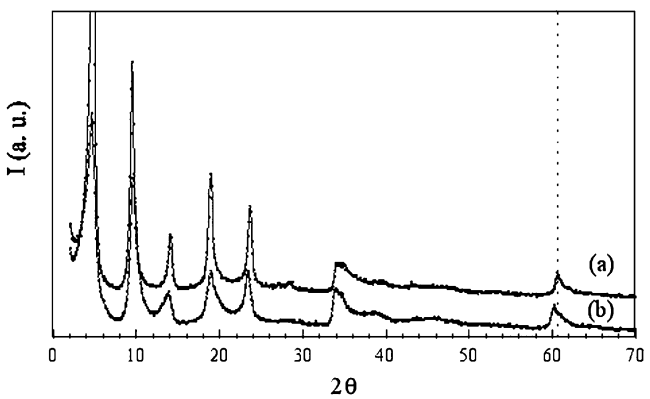

Figure 1. XRD patterns of the hybrid phases Zn_nAl/SPMA samples: (a) n = 2, and (b) n = 3.

The observed difference of $\Delta\boldsymbol{a} = 1.6 \times 10^{-3}$ nm is in agreement with the variation of the layer charge between the two hybrid phases, thus further supporting the cation ratio values.[26] About six harmonic lines are observed on the XRD patterns. The corresponding d spacing is 1.87 nm in both cases. It is commonly accepted that a lowering of the layer charge (n: 2 → 3) induces an increase of the interlayer space, with the electrostatic forces between anions and layers becoming weaker. The fact that the d spacing is here unchanged may be interpreted by the size and the hydrophilic/hydrophobic nature of the surface active monomer SPMA. The crystallinity is, however, different between the two phases, as Zn_2Al/SPMA presents sharper (00l) diffraction lines than Zn_3Al/SPMA. The former corresponds to a greater number of stacked platelets, which is usually the trend observed when the layer charge is decreased.[9]

Concerning the guest molecule, its size along the carbon backbone is estimated to be 1.05 nm from semiempirical Hartree−Fock calculations (Spartam program). In the hypothesis of SPMA lying perpendicularly to the sheets and considering the brucitic layer width, it leaves some free space, which has to be interpreted by the repulsion between the methyl terminal group and the LDH sheets. However, the value of the d spacing is not sufficient to unambiguously determine the arrangement of the organic molecule, as it may be tilted from the vertical position. Nevertheless it suggests an interdigitation of the interleaved surfactant molecules.

3.2. Interaction between SPMA and LDH Sheets. FTIR spectra of SPMA and the hybrid phase Zn_2Al/SPMA are displayed in Figure 2. Most of the vibration bands of SPMA may be attributed as follows: the stretching vibrations C=O and C=C occurring at 1720 and 1636 cm^{-1}, respectively, and the vibrations assigned to the methyl and methylene groups appear in the domain 2900−3000 cm^{-1}. IR bands are further assigned in the following according to the literature.[27] The

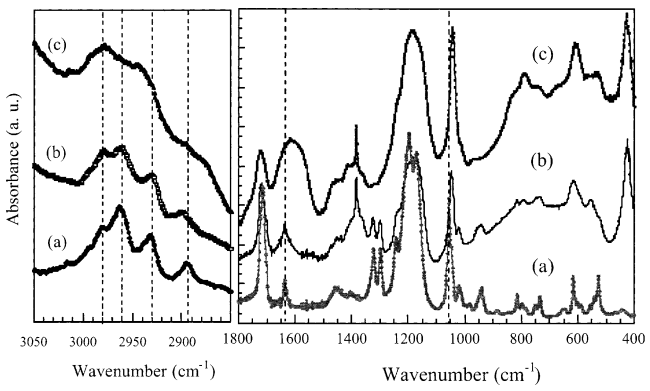

Figure 2. FTIR spectra of (a) SPMA-K salt and of the hybrid phase Zn_2Al/SPMA (b) before and (c) after thermal treatment. The positions of the stretching S=O and C=C are shown by dashed lines (see text). In the left part, the domain of vibration bands CH_2 and CH_3 is enlarged.

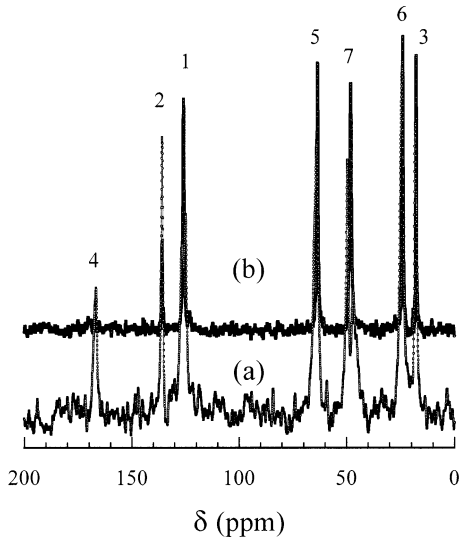

Figure 3. ^{13}C CP-MAS NMR spectra of (a) SPMA-K salt and (b) Zn_2Al/SPMA. The labeling is according to $H_2{}^1C = {}^2C({}^3CH_3)\text{-}{}^4CO_2{}^5CH_2{}^6CH_2{}^7CH_2SO_3$(K or LDH).

absorption band at 950 cm^{-1} is assigned to C=C−C=O. Because the SPMA molecule is tethered via its sulfonate group, any electrostatic interaction between the sulfonate group and the inner surface of LDH should be associated with a shift of the corresponding vibration bands. The symmetric stretching S=O located at 1059 cm^{-1} for SPMA is downshifted to 1046 cm^{-1} for the hybrid phase. This shift constitutes clear evidence that a geometric disturbance of the functional group (SO_3^-) is occurring, which in our case corresponds to a weakening of the S=O bond strength. The loosening of the S=O bond suggests the presence of an electrostatic binding with the clay surface through a hydrogen bond via a path S=O···H−O−M (M = Al or Zn).

Other evidences of interactions between SPMA and the clay may be provided by solid-state NMR spectroscopy. ^{13}C NMR resonance peaks observed on the spectrum of SPMA−K salt are assigned as shown in Figure 3. The vinyl carbon C^2 is located at 135.9 ppm, for the C^1, its contribution is split into two peaks at 126.7 and 125.1 ppm. The splitting (of 120. 8 Hz), which is no longer observed in the case of the hybrid phase, may be due to $^{13}C-{}^1H$ heteronuclear coupling. The same trend is observed for C^3, C^5, and C^6, and the peak splitting is also canceled once SPMA is incorporated between LDH sheets. The resonance peak of C^4 is not observed for the hybrid phase. For C^7, an upfield shift is observed. This is consistent with an electrostatic interaction of the SO_3 function with the LDH surface, thus involving mostly the carbon nucleus C^7 close to the functional group. The shielding effect is not propagated through the monomer backbone, as the alkyl chain is here strongly mitigating such an effect as observed for other surfactant molecules.[9] Conversely, in the case of styrene sulfonate[9] the propagation is observed; we think that the electronic delocalization present in the benzene ring may act as a relay.

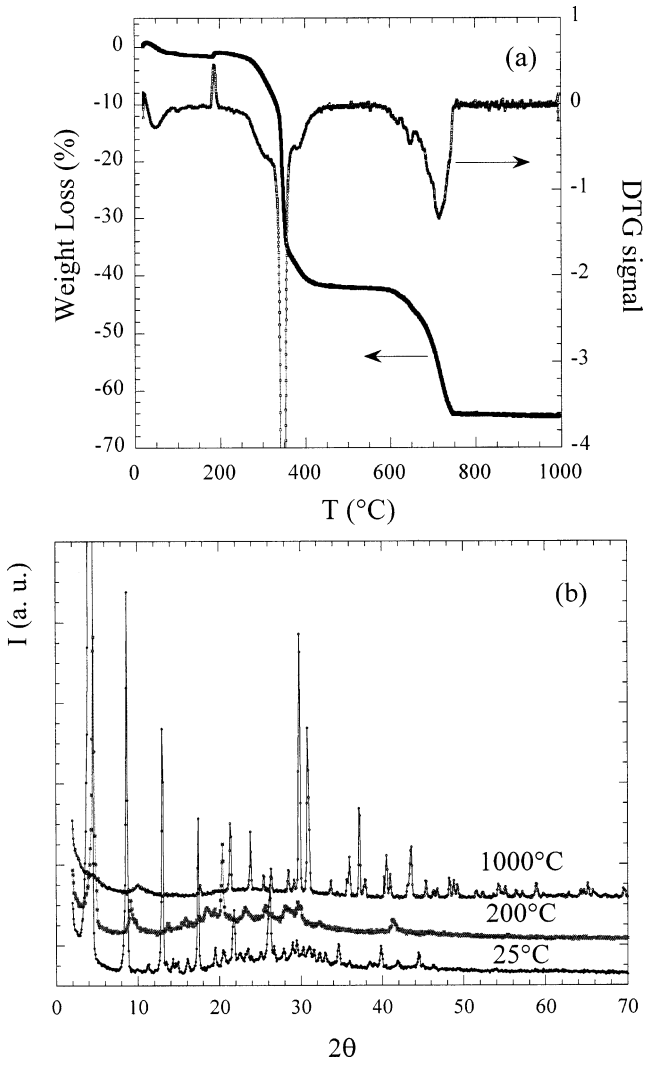

Figure 4. Thermal behavior of SPMA: (a) TG analysis under air, and (b) XRD patterns recorded at different temperatures.

Additionally, the interaction between SPMA and the host structure is also manifested on the FTIR spectrum by a shift of the band assigned to the methylene group. In the domain 2850−2950 cm^{-1}, the symmetric and antisymmetric stretching vibrations of CH_2 and CH_3 occur. One of the four vibration bands is shifted to higher wavenumber (2894 → 2900 cm^{-1}) (Figure 2, left part); we surmise that this corresponds to the methylene group directly attached to the sulfonate. It was possible to ascertain such an effect because the peaks are isolated.

The presence of vibration bands due to the inorganic structure (M−O, and O−M−O) makes difficult any analysis in the domain 400−900 cm^{-1}, where the vibration of the bond C−S is located.

3.3. Behavior in Temperature. *3.3.a. SPMA Potassium Salt.* Figure 4a shows the thermal behavior of SPMA. In the inset, a well-pronounced DTG signal is observed. It corresponds to an exothermic peak on the heat flow curve associated with a slight gain of mass (Figure 5). X-ray diagrams of SPMA at 25 °C and after thermal treatment at 200 and 1000 °C for 2 h are presented in Figure 4b. From these results, we conclude that SPMA exhibits a lamellar structure at room temperature, which is consistent with a lipidic-type arrangement of the surface active monomer. After

(26) Leroux, F.; Adachi-Pagano, M.; Intissar, M.; Chauvière, S.; Forano, C.; Besse, J.-P. *J. Mater. Chem.* **2001**, *11*, 105.
(27) Belfer, S.; Fainchtain, R.; Purinson, Y.; Kedem, O. *J. Membr. Sci.* **2000**, *172*, 113.

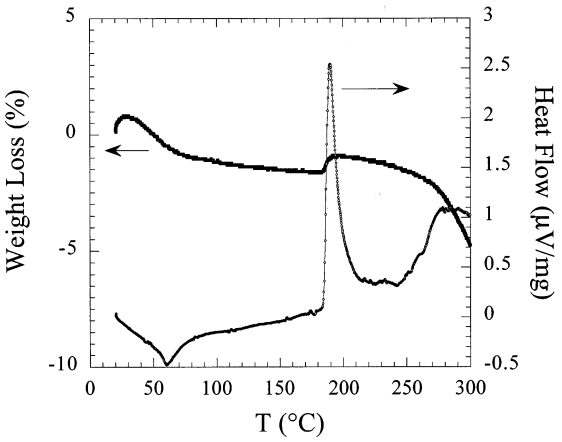

Figure 5. Thermal behavior of SPMA in the lower temperature domain (T < 300 °C).

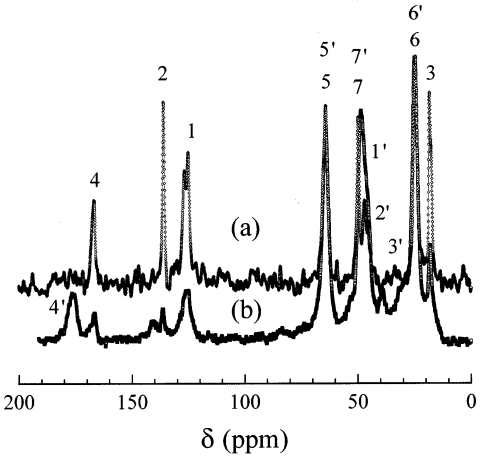

Figure 6. ^{13}C CP-MAS NMR spectra of SPMA (a) before and (b) after thermal treatment at 200 °C for 2 h. The labeling is according to $H_2{}^1C = {}^2C({}^3CH_3)^4CO_2{}^5CH_2{}^6CH_2{}^7CH_2SO_3(K)$ and $-H_2{}^{1'}C\text{-}{}^{2'}C({}^{3'}CH_3)^{4'}CO_2{}^{5'}CH_2{}^{6'}CH_2{}^{7'}CH_2SO_3(K)$.

treatment at 200 °C, the spacing between organic layers decreases from 2.07 to 1.91 nm, suggesting that the alkyl chains are slightly more interdigitated. After the loss of its organic component, SPMA decomposes into K_2SO_4 (PDF 5-0613, arcanite). The final weight loss is in agreement with the following decomposition process:

$$2\ \text{SPMA-K} \rightarrow K_2SO_4\ (\Delta m/m_{th} = 64.6\%,\ \Delta m/m_{exp} = 64\%)$$

To know whether the thermal event observed at 190 °C associated with the small contraction of the lipidic-like structure and the slight gain of mass was accompanied by a polymerization process, ^{13}C CP-MAS spectrum was recorded (Figure 6). The resonance peak of carbon nuclei C^6 and C^5 is not modified, whereas the intensity of C^1, C^2, and C^3 is strongly decreased, and concomitantly, an additional resonance peak appears at 176.1 ppm. One has to note that the CP sequence is not quantitative, however, the same number of scans was applied for SPMA before and after thermal treatment. The change observed on the spectrum has to be interpreted by the opening of the double band, thus decreasing the vinyl carbons nuclei response (C^1 and C^2). This affects also C^4, which is deshielded, and the shoulder observed for the resonance peaks C^7 and C^6 may be attributed to C^1 and C^3, respectively, once the monomer is partially polymerized. Thermal treatment using longer time does not convert significantly more monomers into poly(SPMA).

The polymerization process may be interpreted as an oxidative reaction induced by the oxygen molecules, thus explaining the slight gain of mass occurring at this temperature (Figure 5).

3.3.b. Hybrid Phases. Powder X-ray diffraction patterns were recorded in-situ in a range of temperatures (Figure 7). The lamellar structure is found to decrease progressively from 1.9 to 1.7 nm in temperature until 200 °C (the temperature at which the stacking sequence is barely observed anymore) while the sheets are unmodified, as evidenced by the conservation of the diffraction line (110). To know the origin of such a disagglomeration-like process, further characterizations were performed.

^{13}C CP-MAS spectrum of Zn_2Al/SPMA was recorded after treatment at 200 °C (Figure 8). As observed, the vinyl carbon response has completely disappeared, as well as the resonance peak of C^3. At the same time, a large shoulder is observed at around 26 ppm, and the

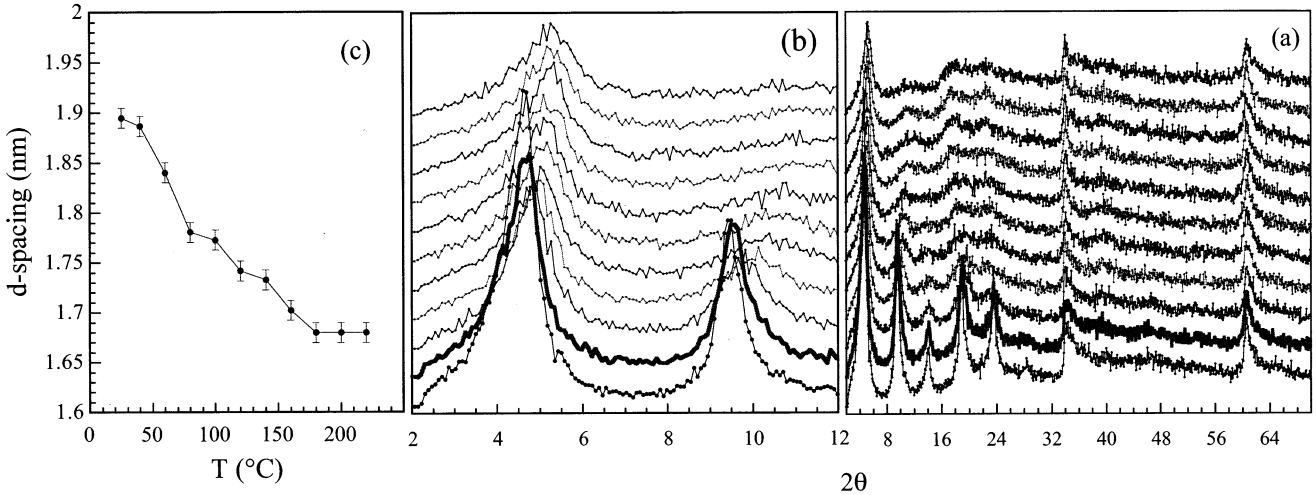

Figure 7. In situ XRD patterns of the hybrid phase Zn_2Al/SPMA recorded every 20 °C from room temperature up to 220 °C: (a) 2θ angular domain from 2 to 70°, (b) low-2θ domain enlarged for clarity, and (c) variation of the basal spacing with temperature.

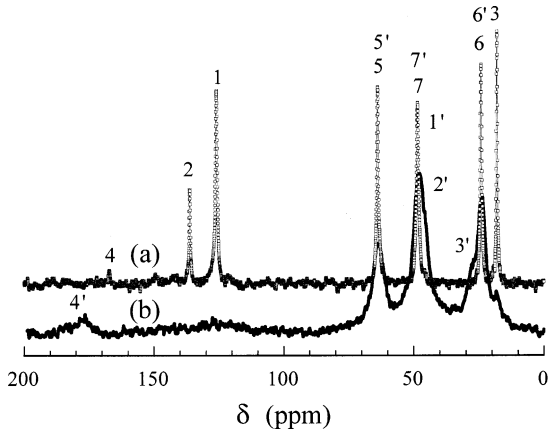

Figure 8. ^{13}C CP-MAS NMR spectra of the hybrid phase Zn_2-Al/SPMA (a) before and (b) after thermal treatment at 200 °C for 2 h. The labeling is according to $H_2{}^1C = {}^2C({}^3CH_3){}^4CO_2$-${}^5CH_2{}^6CH_2{}^7CH_2SO_3$ (LDH) and $-H_2{}^{1'}C$-${}^{2'}C({}^{3'}CH_3){}^{4'}CO_2{}^{5'}CH_2$-${}^{6'}CH_2{}^{7'}CH_2SO_3$ (LDH).

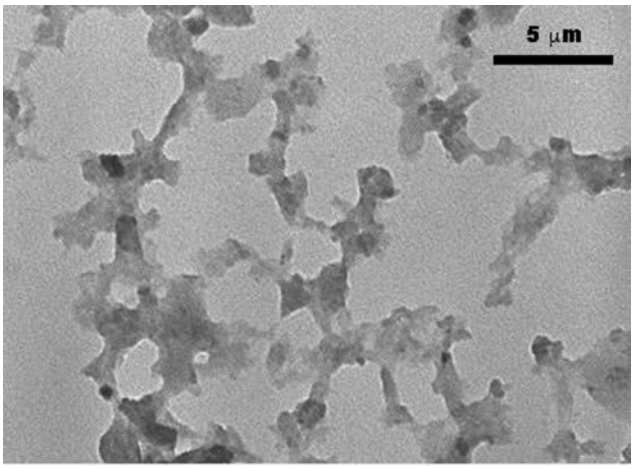

Figure 9. TEM pictures of the hybrid phase Zn_2Al/SPMA after thermal treatment at 200 °C for 2 h. The magnification is indicated.

position of C^4 is now located at 176.1 ppm, similarly to SPMA-K salt after thermal treatment. The quaternary carbon C^2 is expected in the range 40−50 ppm, supposedly in the shoulder of the resonance peak located at 49 ppm. All these changes demonstrate that the polymerization is not *partial* but *total* when SPMA is located between the sheets, thus underlining the importance of the constrainment supplied by the host structure.

The temperature affects the IR spectrum by broadening the vibration bands (Figure 2c). For instance, a large contribution is located at 1600 cm^{-1}, and the narrow vibration band assigned to C=C has disappeared. The vibration bands of CH_2 and CH_3 are lumped together, impeding any further assignments. The lattice vibration bands are mostly unaffected, in agreement with the conservation of the LDH sheets.

The hybrid phase without thermal treatment reacts under the beam. White spots appear rapidly, and after a few seconds the exposed particles are broken down. We explain this phenomenon by the polymerization of the acrylate-based monomer under the electron beam. The hybrid phase after thermal treatment at 200 °C is stable under the beam, and is composed of isolated

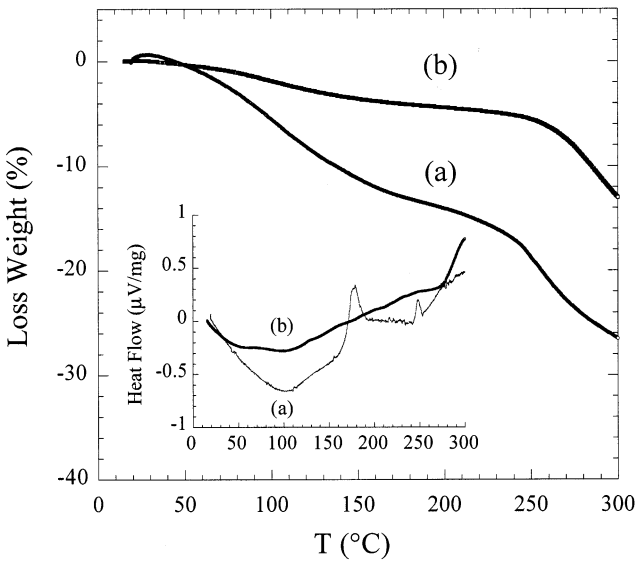

Figure 10. Thermal behavior (T < 300 °C) of the hybrid phase Zn_2Al/SPMA (a) before and (b) after thermal treatment at 200 °C. The corresponding heat flow curves are displayed in the inset.

particles of submicron size (≈400−500 nm) (Figure 9). Thus, we may picture the effect of the polymerization of interleaved SPMA acting to contract the layers, but also to disagglomerate the lamellar structure.

The thermal behavior of the hybrid phase was studied (Figure 10). In the inset of Figure 10, the heat flow curves are displayed. The exothermic peak assigned to the polymerization of SPMA is shifted to lower temperature, from 190 to 176 °C, when the organic molecule is confined into the LDH gap; this process is absent after the thermal treatment at 200 °C. We observed that the thermal events occurring at higher temperature are dependent on the thermal treatment used for the polymerization reaction. A longer time (2 h versus a few minutes used for the TG analysis) delays the temperature of degradation of the organic moiety. Because it must be related to the polymer chains formation, we surmise that the polymerization is kinetically limited, this was also underlined for other interleaved vinyl-based monomer[9] or conductive polymer.[12c]

4. Conclusion

For the first time, a surface active monomer (SPMA) was incorporated into LDH structure using the coprecipitation method. The study provides clear evidences of the in situ polymerization of SPMA into LDH gap by thermal treatment. When the surface active monomer is confined, the reaction is complete without the use of any external chemical agent. Nevertheless, the thermal behavior of the free SPMA molecules suggests that the oxygen molecules may act as an external initiator for the polymerization. A study of the thermal behavior suggests strongly that the polymerization is kinetically limited.

Acknowledgment. We thank Dr. Vanessa Prévot (LMI) for the TEM pictures.

CM040165X